

Application of Strain Energy Density and Maximum Circumferential Stress Criteria to Dynamic Crack Curving

A. SHUKLA*, R. CHONA** and C. ZHU*

**Department of Mechanical Engineering and Applied Mechanics,
The University of Rhode Island, Kingston, RI 02881, USA*

***Mechanical Engineering Department, Texas A&M University,
College Station, TX 77843, USA*

ABSTRACT

Dynamic photoelastic experiments were conducted to provide information regarding the state of stress associated with a rapidly curving crack. Analysis of the crack tip isochromatic patterns permitted evaluation of both the singular and non singular components of the mixed mode stress field over a region of reasonable size around the crack tip at various positions along the crack path. The stress field coefficients obtained were then used to predict the direction of the next segment of crack extension using the strain energy density and the maximum circumferential stress criteria. This predicted crack path was compared with the experimental data and showed good agreement.

KEYWORDS

Strain energy density, maximum circumferential stress, dynamic crack curving, stress intensity factor, photoelasticity.

INTRODUCTION

Trajectory problems in mechanics, such as the problem of determining the path followed by a particle in a potential field such that it traverses the distance between two points in the shortest time (the brachistochrone problem first considered by Bernoulli), have long been recognized as being complex [1]. The problem of prediction of the crack path in fracture mechanics is no less so, even when attention is restricted to a two-dimensional planar crack that is propagating at a constant speed [2].

The solution to the general crack trajectory problem requires: (a) the computation of the stress intensity factors and other related stress field parameters for a given crack in an arbitrary body at any instant in time; and

(b) a means of defining the next increment of crack growth in terms of geometrical parameters that are related to the previously computed information about the crack tip stress field. The solution to this problem has been attempted by a number of researchers for certain special cases, using either closed-form, quasi-static, analytical solutions, or numerical techniques to compute the small change of direction for each forward increment of crack extension based on the maximization of the normal tensile stress ahead of the crack tip [3].

The aim of the present work was to examine the path followed by the crack relative to the stress field in the local region surrounding the crack tip. This was done by first carefully evaluating the magnitude of both the singular and the leading non-singular stress and strain components of the crack-tip stress field for cracks propagating along smoothly curving paths in a brittle, isotropic material, and then examining the crack path relative to the magnitude of both the singular and non-singular stress field parameters.

The approach adopted here has been to use dynamic photoelasticity and a high speed camera system of the Cranz-Schardin type to obtain full-field information about the stress state surrounding the tip of a crack propagating in a plate specimen fabricated from a brittle, birefringent polymer.

The resulting information was in the form of isochromatic fringe patterns, or contours of constant maximum in-plane shear stress, which provided the data base for further analyses. Local collocation procedures were then employed, in which the appropriate stress field representations for running cracks were combined with a multiple data point, overdeterministic, non-linear algorithm to obtain the stress field parameters of interest in a least squares sense [4,5,6]. These stress field parameters were then used to predict the direction of the next segment of crack extension using the strain energy density [7] and the maximum circumferential stress criteria [8].

Dynamic Crack Tip Stress Field Equations

It has been previously shown [9,10] that the mixed mode stress field associated with a crack propagating at a constant velocity, c , is given in terms of the local rectangular coordinates by

$$\sigma_{xx} = \frac{(1+\lambda_2^2)}{4\lambda_1\lambda_2 - (1+\lambda_2^2)^2} \left\{ (1 + 2\lambda_1^2 - \lambda_2^2) \text{Re } Z_1 - \frac{4\lambda_1\lambda_2}{1+\lambda_2^2} \text{Re } Z_2 + \right. \\ \left. + (1+2\lambda_1^2 - \lambda_2^2) \text{Re } Y_1 - (1+\lambda_2^2) \text{Re } Y_2 \right\} + \frac{2\lambda_2}{4\lambda_1\lambda_2 - (1+\lambda_2^2)^2} \\ \left\{ (1+2\lambda_1^2 - \lambda_2^2) \text{Re } Y_1^* - \frac{4\lambda_1\lambda_2}{1+\lambda_2^2} \text{Re } Y_2^* + (1+2\lambda_1^2 - \lambda_2^2) \text{Re } Z_1^* - (1+\lambda_2^2) \text{Re } Z_2^* \right\} \quad (1)$$

$$\sigma_{yy} = \frac{(1+\lambda_2^2)}{4\lambda_1\lambda_2 - (1+\lambda_2^2)^2} \left\{ - (1+\lambda_2^2) \text{Re } Z_1 + \frac{4\lambda_1\lambda_2}{1+\lambda_2^2} \text{Re } Z_2 - \right.$$

$$\left. - (1+\lambda_2^2) \text{Re } Y_1 + (1+\lambda_2^2) \text{Re } Y_2 \right\} + \frac{2\lambda_2}{4\lambda_1\lambda_2 - (1+\lambda_2^2)^2} \\ \left\{ - (1+\lambda_1^2) \text{Re } Y_1^* + \frac{4\lambda_1\lambda_2}{1+\lambda_2^2} \text{Re } Y_2^* - (1+\lambda_2^2) \text{Re } Z_1^* + (1+\lambda_2^2) \text{Re } Z_2^* \right\} \quad (2)$$

$$\tau_{xy} = \frac{(1+\lambda_2^2)}{4\lambda_1\lambda_2 - (1+\lambda_2^2)^2} \left\{ - 2\lambda_1 \text{Im } Z_1 + 2\lambda_1 \text{Im } Z_2 - 2\lambda_1 \text{Im } Y_1 + \right. \\ \left. + \frac{(1+\lambda_2^2)^2}{2\lambda_2} \text{Im } Y_2 \right\} + \frac{2\lambda_2}{4\lambda_1\lambda_2 - (1+\lambda_2^2)^2} \left\{ - 2\lambda_1 \text{Im } Y_1^* + 2\lambda_1 \text{Im } Y_2^* - \right. \\ \left. - 2\lambda_1 \text{Im } Z_1^* + \frac{(1+\lambda_2^2)^2}{2\lambda_2} \text{Im } Z_2^* \right\} \quad (3)$$

with

$$Z_1 = \sum_{n=0}^N A_n z_1^{n-1/2} \quad \text{and} \quad Z_2 = \sum_{n=0}^N A_n z_2^{n-1/2} \quad (4)$$

$$Y_1 = \sum_{m=0}^M B_m z_1^m \quad \text{and} \quad Y_2 = \sum_{m=0}^M B_m z_2^m \quad (5)$$

$$Z_1^* = \sum_{n=0}^N -i C_n z_1^{n-1/2} \quad \text{and} \quad Z_2^* = \sum_{n=0}^N -i C_n z_2^{n-1/2} \quad (6)$$

$$Y_1^* = \sum_{m=0}^M -i D_m z_1^m \quad \text{and} \quad Y_2^* = \sum_{m=0}^M -i D_m z_2^m \quad (7)$$

where λ_1 , λ_2 , z_1 and z_2 are coordinate parameters defined in Fig. 1.

The leading coefficient in Z_1 and Z_2 , A_0 , is related to the opening mode stress intensity factor K_I , $K_I = A_0/2\pi$. The first coefficient in Z_1^* and Z_2^* , C_0 , is related to the shear mode stress intensity factor $K_{II} = C_0/2\pi$. The leading term in Y_1 and Y_2 , B_0 , gives rise to the superposed constant stress in the direction of crack propagation and is related to the familiar σ_{ox} term by $\sigma_{ox} = 2B_0$. The first term in series Y_1^* and Y_2^* , D_0 , does not influence the stress field and as such cannot be determined from stress-based information.

Minimum Strain Energy Density Criterion

The strain energy density criterion proposed by Sih [7] states that crack growth takes place in the direction of minimum strain energy density. The strain energy density, W , per unit volume, V , for plane stress conditions is given by

$$\frac{dW}{dV} = \frac{1}{2E} (\sigma_x^2 + \sigma_y^2) - \frac{\nu}{E} \sigma_x \sigma_y + \frac{(1+\nu)}{E} \tau_{xy}^2 \quad (8)$$

where E and ν are the elastic modulus and Poisson's ratio respectively. In

order to evaluate the direction of the propagating crack the density of the strain energy at a core radius r_c is minimized. Thus the direction of crack propagation is obtained by

$$\frac{d}{d\theta} \left[r_c \frac{dW}{dV} \right] = 0 \quad \text{and} \quad \frac{d^2}{d\theta^2} \left[r_c \frac{dW}{dV} \right] > 0 \quad (9)$$

Maximum Circumferential Stress Criterion

The maximum circumferential stress criterion postulates that crack extension takes place in the direction perpendicular to the direction of maximum tensile principal stress. The circumferential stress σ_θ will be the principal stress if the shear stress $\tau_{r\theta} = 0$. Thus to obtain the direction of crack propagation

$$\tau_{r\theta} = 0 = \frac{1}{2} (\sigma_y - \sigma_x) \sin 2\theta + \tau_{xy} \cos 2\theta \quad (10)$$

where eq. 10 is also evaluated at $r = r_c$.

RESULTS AND DISCUSSION

Dynamic photoelasticity was used to record the isochromatic fringes associated with a crack propagating along a curved path. Two experiments were performed and the photographs are shown in Figs. 2 and 3. The details of the experimental procedure and the model geometry are given in Ref. 11. In both the experiments the cracks propagated at a constant velocity of 380 m/sec. The photoelastic data were analyzed using the multipoint overdeterministic method [4,5,6]. Good results with very low fringe order errors (~3-5%) were obtained with five terms in each series for the stress field representation [10].

Figure 4 shows the variation of the stress intensity factors as a function of time for both the experiments. Mode I stress intensity factor shows a large value of K_I varying from 1.3 to 1.6 MPa/m as the crack propagates across the model. Mode II stress intensity factor, K_{II} , on the other hand consistently shows a very small value, close to zero, throughout. Figures 5, 6 and 7 show the variation of the higher order terms with time after crack initiation. It is interesting to note that the values of the higher order term are not random but show a smooth trend with crack propagation.

The experimental results thus obtained for both the experiments were used to evaluate the state of stress (σ_{xx} , σ_{yy} and τ_{xy}) around the propagating crack tip. Knowing the dynamic state of stress, the instantaneous direction of crack propagation was obtained at discrete times using the strain energy density and the maximum circumferential criteria. The results are shown in Figs. 8 and 9. The crack path predictions from both the criteria match well with the actual crack path. It should be mentioned that the results are sensitive to the choice of the core radius, r_c . The value of r_c used in these calculation is the one suggested by Ramulu and Kobayashi [12]. This also happens to be the value which gives the best results for crack path.

CONCLUSIONS

1. The results show that for a rapidly curving crack the shear mode

stress intensity factor is zero or close to zero, and does not vary with changes in the crack trajectory.

2. Non singular stress field coefficients for both mode I and mode II series vary in a systematic fashion as the crack propagates across the model.
3. The crack path predictions from both the strain energy density and the maximum circumferential stress criteria match well with the experimental data.

ACKNOWLEDGEMENT

The authors would like to acknowledge the support of NSF under grant no. MSM-8719567.

REFERENCES

1. Goldstein, H., Classical Mechanics, Addison-Wesley Publishing Company, Reading, Massachusetts (1959).
2. Freund, L.B., "Dynamic Crack Propagation in Solids", in Computational Methods in the Mechanics of Fracture, S.N. Atluri, editor, North-Holland Publishing Company, New York, pp. 85-120 (1986).
3. Swenson, D. and A.R. Ingraffea, "A Finite Element Model of Dynamic Crack Propagation with an Application to Intersecting Cracks", Proceedings of the Fourth International Conference on Numerical Methods in Fracture Mechanics, A.R. Luxmoore, et al., editors, Pineridge Press, Swansea, U.K., pp. 191-204 (1987).
4. Sanford, R.J. and J.W. Dally, "A General Method for Determining Mixed Mode Stress Intensity Factors from Isochromatic Fringe Patterns", Engineering Fracture Mechanics, 11, pp. 621-633 (1979).
5. Sanford, R.J., "Application of the Least-Squares Method to Photoelastic Analysis", Experimental Mechanics, 20, pp. 192-197 (1980).
6. Chona, R., The Stress Field Surrounding the Tip of a Crack Propagating in a Finite Body, Ph.D. Dissertation, University of Maryland, Advisor: G.R. Irwin (1987).
7. Sih, G.C., "Some Basic Problems in Fracture Mechanics and New Concepts", Engr. Fracture Mechanics, Vol. 5, pp. 365-377 (1973).
8. Erdogan, F. and Sih, G.C., "On the Crack Extension in Plates Under Plane Loading and Transverse Shear", J. Basic Engr., 85 pp. 519-527 (1963).
9. Nishioka, T. and Atluri, S.N., "Path Independent Integrals, Energy Release Rates and General Solutions of Near-Tip Fields in Mixed Mode Dynamic Fracture Mechanics", Engr. Fracture Mechanics, Vol. 18, pp. 1-22 (1983).
10. Shukla, A. and Chona, R., "The Stress Field Surrounding a Rapidly Propagating Curving Crack", Fracture Mechanics: Eighteenth Symposium, ASTM STP 945, pp. 86-99 (1988).
11. Shukla, A. and Anand, S., "Dynamic Crack Propagation and Branching Under Biaxial Loading", Fracture Mechanics: Seventeenth Symposium, ASTM STP 905, pp. 697-714 (1986).
12. Ramulu, M. and Kobayashi, A.S., "Strain Energy Density Criteria for Dynamic Fracture and Dynamic Crack Branching", Theoretical and Applied Fracture Mechanics, 5, pp. 117-123 (1986).

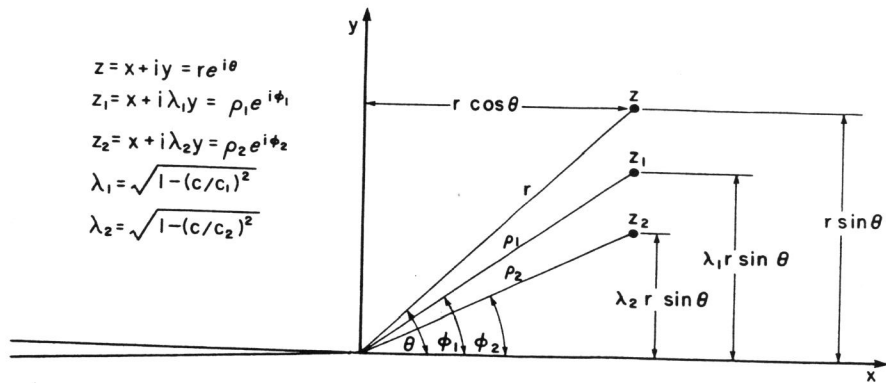


Fig. 1 Crack tip coordinate system.

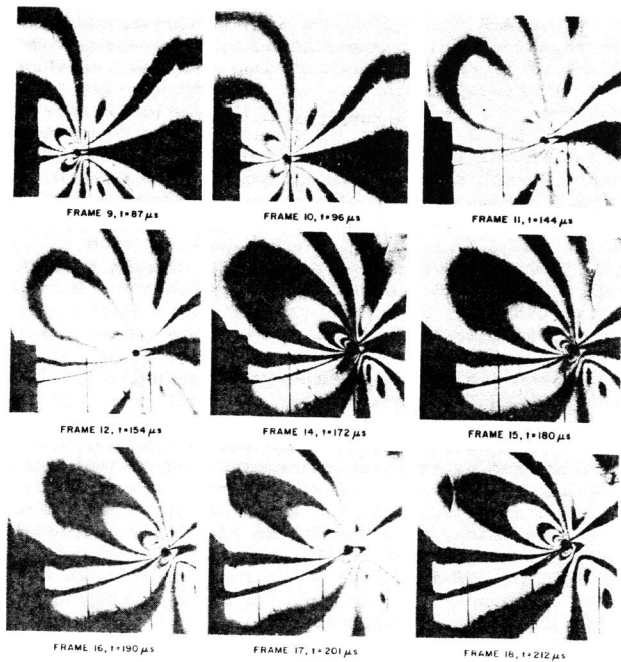


Fig. 2 Dynamic isochromatic fringes associated with a curving crack.

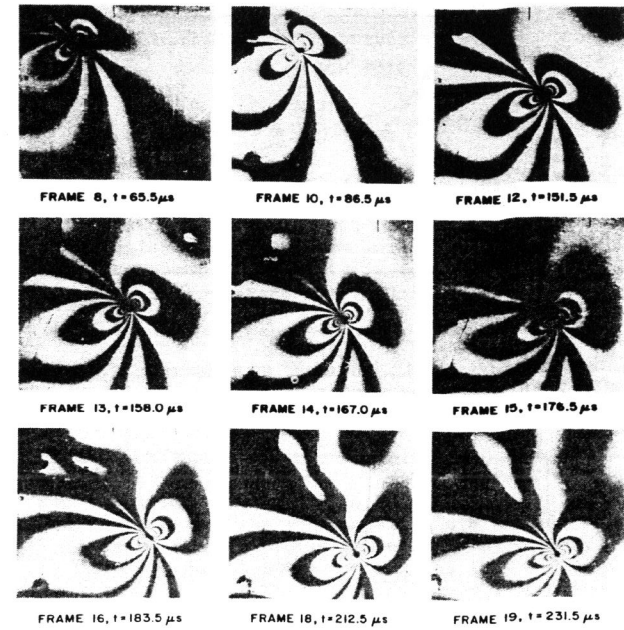


Fig. 3 Dynamic isochromatic fringes associated with a curving crack.

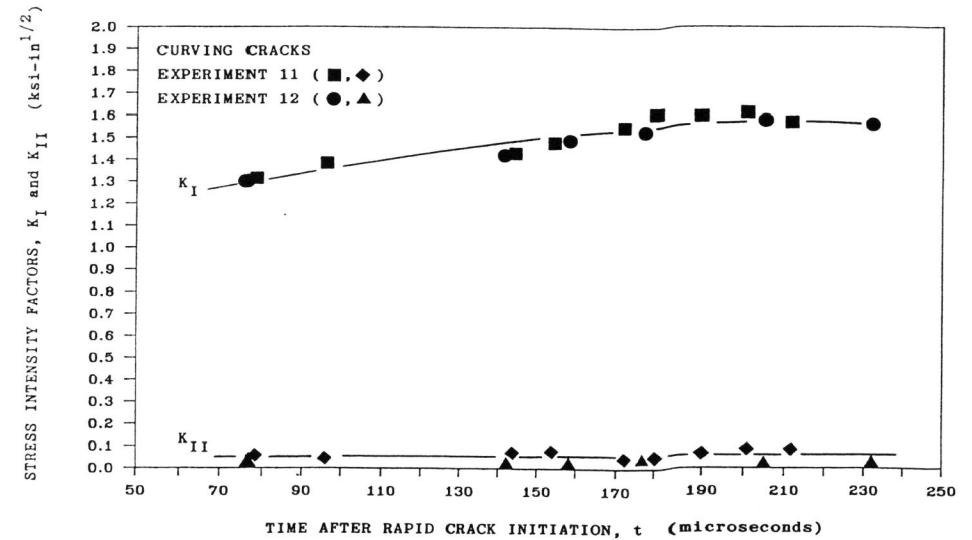


Fig. 4 Stress intensity factors, K_I and K_{II} , as functions of the elapsed time after rapid crack initiation.

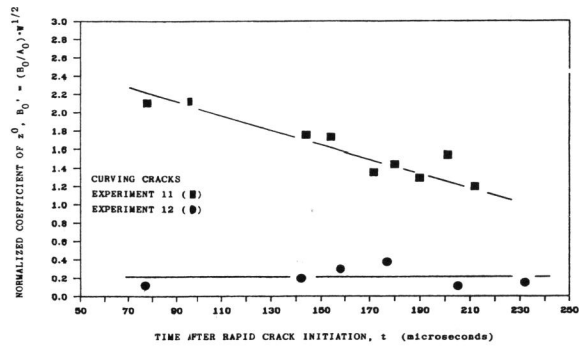


Fig. 5 The normalized coefficient of Z^0 as a function of the elapsed time after rapid crack initiation.

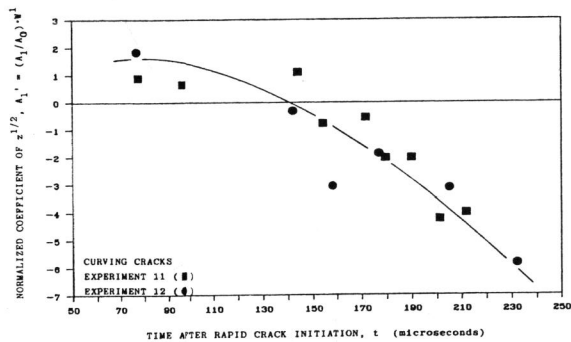


Fig. 6 The normalized opening mode coefficient of $Z^{1/2}$ as a function of the elapsed time after rapid crack initiation.

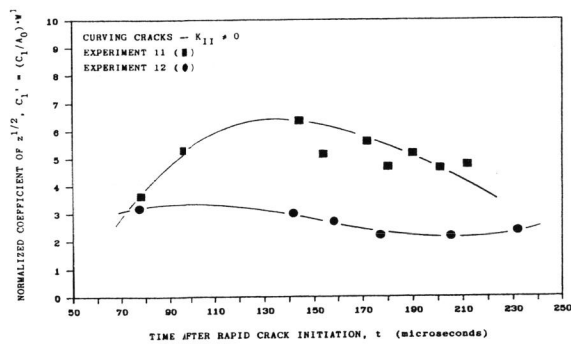


Fig. 7 The normalized shear mode coefficient of $Z^{1/2}$ as a function of the elapsed time after rapid crack initiation.

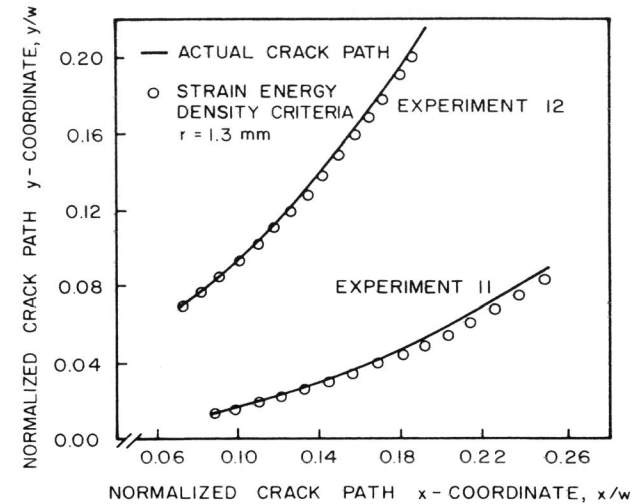


Fig. 8 Comparison of the actual crack path with the results predicted from the minimum strain energy density criterion.

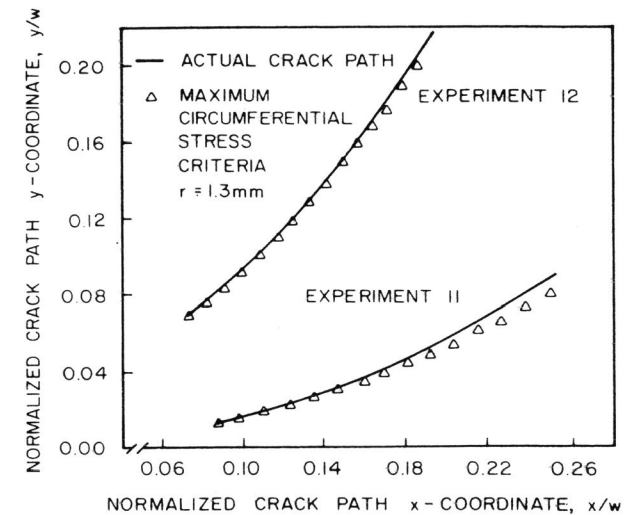


Fig. 9 Comparison of the actual crack path with the results predicted from the maximum circumferential stress criterion.